

15-267217 Y

NASA CR-120854



TOPICAL REPORT

THERMAL CONDUCTIVITY AND ELECTRICAL RESISTIVITY OF POROUS MATERIAL

BY

J. C. Y. KOH, The Boeing Company

ANTHONY FORTINI, NASA-Lewis Research Center

PREPARED FOR

NATIONAL AERONAUTICS AND SPACE ADMINISTRATION

OCTOBER 1971

CONTRACT NAS 3-12012

THE **BOEING** COMPANY
AEROSPACE GROUP
SEATTLE, WASHINGTON

(NASA-CR-120854) THERMAL CONDUCTIVITY AND
ELECTRICAL RESISTIVITY OF POROUS MATERIAL
J.C.Y. Koh, et al (Boeing Co.) Oct. 1971
49 p

572-12-36

CRCT 115

Index

33/19 21-11

FACILITY
CR-120854
(NASA CR OR TMX OR AD NUMBER)

18
(CATEGORY)



NASA CR-120854



TOPICAL REPORT

**THERMAL CONDUCTIVITY AND ELECTRICAL
RESISTIVITY OF POROUS MATERIAL**

BY

J. C. Y. KOH, The Boeing Company

ANTHONY FORTINI, NASA—Lewis Research Center

PREPARED FOR

NATIONAL AERONAUTICS AND SPACE ADMINISTRATION

OCTOBER 1971

CONTRACT NAS 3-12012

THE **BOEING** COMPANY
AEROSPACE GROUP
SEATTLE, WASHINGTON

ABSTRACT

Thermal conductivity and electrical resistivity of porous materials, including 304L stainless steel Rigidmesh, 304L stainless steel sintered spherical powders, and OFHC sintered spherical powders at different porosities and temperatures are reported and correlated. It was found that the thermal conductivity and electrical resistivity can be related to the solid material properties and the porosity of the porous matrix regardless of the matrix structure. It was also found that the Wiedermann-Franz-Lorenz relationship is valid for the porous materials under consideration. For high conductivity materials, the Lorenz constant and the lattice component of conductivity depend on the material and are independent of the porosity. For low conductivity, the lattice component depends on the porosity as well.

TABLE OF CONTENT

	Page No.
ABSTRACT	ii
1.0 INTRODUCTION	1
2.0 MATERIALS STUDIED	1
3.0 RESULTS AND DISCUSSIONS	2
3.1 THERMAL CONDUCTIVITY	2
3.2 ELECTRICAL RESISTIVITY	3
3.3 TEMPERATURE EFFECTS	3
3.4 DIMENSIONLESS CONDUCTIVITY AND RESISTIVITY	4
3.5 RELATION BETWEEN THERMAL CONDUCTIVITY AND ELECTRICAL RESISTIVITY	6
4.0 PREDICTION OF THERMAL CONDUCTIVITY OF POROUS MATERIALS	9
4.1 PREDICTION OF POROUS MATERIAL CONDUCTIVITY FROM SOLID CONDUCTIVITY DATA	9
4.2 PREDICTION OF POROUS MATERIAL CONDUCTIVITY FROM ELECTRICAL RESISTIVITY DATA	9
5.0 CONCLUSIONS AND RECOMMENDATIONS	10
5.1 CONCLUSIONS	10
5.2 RECOMMENDATIONS	10
6.0 REFERENCE	11
NOMENCLATURE	13
TABLES	14 - 21
FIGURES	22 - 33
APPENDIX A - NUMERICAL EXAMPLE	34

LIST OF TABLES

	Page
I Details of Tested Samples	14
II Thermal Conductivity, Electrical Resistivity and Derived Lorenz Function for Porous 304L Stainless Steel	15
(a) Rigimesh	15
(b) Sintered Powders	16
III Thermal Conductivity, Electrical Resistivity and Derived Lorenz Function for Copper Sintered Powders	17
IV Temperature Coefficients	18
V Dimensionless Conductivity and Resistivity of 304L Stainless Steel Rigimesh	19
VI Dimensionless Conductivity and Resistivity of 304L Stainless Steel Sintered Powders	20
VII Dimensionless Conductivity and Resistivity of Copper Sintered Powders	21

LIST OF FIGURES

	Page
1. Thermal Conductivity of Porous 304 and 304L Stainless Steel	22
2. Thermal Conductivity of Copper Sintered Powders	23
3. Electrical Resistivity of Porous 304L Stainless Steel	24
4. Electrical Resistivity of Copper Sintered Powders	25
5. Dimensionless Thermal Conductivity and Electrical Resistivity of Porous Materials	26
6. Comparison of Experimental Data with Correlations of Thermal Conductivity of Porous Materials	27
7. Thermal Conductivity vs. Temperature/Resistivity of Porous 304L Stainless Steel Rigimesh	28
8. Thermal Conductivity vs. Temperature/Resistivity of 304L Stainless Steel Sintered Powders	29
9. Thermal Conductivity vs. Temperature/Resistivity of OFHC Sintered Powders	30
10. Correlation of Thermal Conductivity, Electrical Resistivity, Porosity, and Temperature of 304L Stainless Steel Rigimesh	31
11. Correlation of Thermal Conductivity, Electrical Resistivity, Porosity, and Temperature of 304L Stainless Steel Powders	32
12. Correlation of Thermal Conductivity, Electrical Resistivity, Porosity, and Temperature of 304L Stainless Steel Rigimesh and Powders	33

1.0

INTRODUCTION

Thermal conductivity of porous material is an important property in determining the temperature distribution of coolant and porous structure in transpiration cooling. Due to the irregularity of the microstructures, confident theoretical calculation of thermal conductivity of porous materials is rather difficult if not impossible. Existing prediction methods are based on certain simplifications such as parallel cylinders, laminates in series, spheres dispersed in a conducting medium, etc. Even with a well defined microstructure, the problem remains complex due to the existence of the interface resistance. Therefore, with the exception of parallel cylinders, a semi-empirical approach is the only practical way of predicting the thermal conductivity of porous materials. This approach was used by Grotenhuis, Powell and Tye (Reference 1) who measured the thermal conductivity and electrical resistivity of sintered powder bronze at different porosities ξ from 20°C to 200°C. They found that all the data on thermal conductivity λ and electrical resistivity σ at different temperatures T may be represented by a straight line $\lambda = 2.43 \times 10^{-8} \frac{1}{T} + 2.1$ independent of porosities. They also suggested the use of $\frac{\lambda}{\lambda_0} = 1 - 2.1 \xi$ for thermal conductivity calculations where λ_0 is the thermal conductivity of solid material. Recently, Aivazov and Domashnev (Reference 2) derived an expression for the thermal conductivity of porous materials as follows: $\frac{\lambda}{\lambda_0} = \frac{1-\xi}{1+n\xi^2}$ n is a constant depending on the microstructures. The validity of these expressions for other microstructures and other materials remains unknown. The purpose of the present study is to provide experimental data of thermal conductivity and electrical resistivity of different porous materials at a temperature range from 100°C to 1000°C and to develop semi-empirical equations from these data.

2.0

MATERIALS STUDIED

The materials studied are (1) porous 304L stainless steel Rigimesh, (2) 304L stainless steel sintered spherical-powder, and (3) oxygen free high conductivity copper sintered spherical-powder. For convenience, these materials will be called Rigimesh, stainless powders and copper powders respectively in this report. Three different porosities of each material are investigated. A summary of the tested samples is shown in Table I. In the last column of the Table, the term "Flow" applies to either the heat flow direction in the case of conductivity measurements or the current flow direction in the case of electrical resistivity measurements. For the solid materials and sintered powder samples, the materials are isotropic and the flow is always along the " f " direction designated under column 4. A detailed characterization of the porous materials may be found in References 3, 4 and 5.

The thermal conductivity and electrical resistivity of all samples were measured by Dynatech Corporation. Detailed description of the tests was reported in References 4 and 6.

3.0 RESULTS AND DISCUSSIONS

3.1 THERMAL CONDUCTIVITY

3.1.1 Porous 304L Stainless Steel. The thermal conductivity of porous 304L stainless steel at various porosities and temperatures is shown both in Table II and Figure 1. The effect of thermal expansion on length and area of the sample has not been included. Available data in the literature for solid 304 and 304L stainless steel are also shown in Figure 1 for comparison. Reasonable agreement is found between the published results and the present data. For the same material at various porosities, no valid published data are available for comparison.

Figure 1 shows that at low porosity ($\xi \approx 0.1$), the thermal conductivity of the Rigimesh is significantly higher than that of the sintered powder. This may be due to the experimental error of the Rigimesh.

3.1.2 Porous Copper. The thermal conductivity of copper at various porosities and temperatures is shown in Table III and Figure 2. Several published results of the conductivity of solid copper are also shown in the Figure for comparison. The lines for pure and impure copper were computed by the following equation given in Reference 12.

$$\lambda = \lambda_0 \left[1.05 - .05 \frac{T}{315} \right] \quad (1)$$

where:

$$\lambda_0 = \begin{cases} 414 \text{ w m}^{-1} \text{ k}^{-1} \text{ for pure Cu} \\ 330 \text{ w m}^{-1} \text{ k}^{-1} \text{ for impure Cu} \end{cases}$$

T = Temperature (k)

The present data for the solid copper may be represented by the following equation for the temperature range from 300 K to 1000 K.

$$\lambda = 411.2 \left(1.05 - 0.05 \frac{T}{384.6} \right) \quad (2)$$

Clearly, Figure 2 shows that the conductivity of copper is a significant function of impurity. If it is assumed that the results for pure copper, .9999 Cu and .996 Cu are reliable, then the values of conductivity for .99999 Cu and .999 Cu appear to be too low. In general, it may be stated that within the temperature range from 300 K to 1300 K, the thermal conductivity of porous copper decreases linearly as the temperature increases. Notice that for the porosity of .2096, the thermal conductivity decreases with temperature at a rate significantly higher than at any other porosities. This indicates the possible experimental error for the sample at .2096 porosity.

3.2

ELECTRICAL RESISTIVITY

3.2.1 304L Stainless Steel. The electrical resistivity of porous 304L stainless steel as a function of temperature at various porosity is shown both in Table II and Figure 3. Again, the data have not been corrected for thermal expansion. Published data for the solid material are also shown in the Figure for comparison. For a temperature up to about 900°K, the present results agree with those of Reference 11 quite well. However, for higher temperature the discrepancy is significant. Data from Reference 11 shows a rapid increase of electrical resistivity at a temperature higher than 900°K. This phenomenon is not found in the present data. It is not found in the conductivity information either (Figure 1). In view of the similarity between electrical conductivity and thermal conductivity, it is concluded that the rapid increase of electrical resistivity at the temperature beyond 900°K as shown in Reference 11 may not be valid.

3.2.2 Sintered Powder Copper. The electrical resistivity of copper at various porosities and temperatures are shown in Table III and Figure 4. Resistivity information for solid copper as a function of temperature published in Reference 11 is also shown in the Figure for comparison. Agreement between the present results and those of Reference 11 on solid copper resistivity is quite good.

3.3

TEMPERATURE EFFECTS

The effect of temperature on both the thermal conductivity and electrical resistivity is represented in the form of temperature coefficient in Table IV. The temperature coefficient is computed from the experimental data given in Tables II and III by the following equations:

$$\alpha = \frac{\lambda_T - \lambda_{100}}{T - 100} \quad \frac{1}{\lambda_{100}} = \frac{1}{\Delta T} \left(\frac{\lambda_T}{\lambda_{100}} - 1 \right) \quad (3)$$

$$\beta = \frac{\delta_T - \delta_{100}}{T - 100} \quad \frac{1}{\delta_{100}} = \frac{1}{\Delta T} \left(\frac{\delta_T}{\delta_{100}} - 1 \right) \quad (4)$$

Where the subscript indicates the temperature in degrees C. The temperature coefficients for bronze powders are also shown in Table IV, for comparison. Table IV shows that for the sintered powders the temperature coefficients α and β at 21% porosity is significantly different from the other porosities. As pointed out previously, this may be due to the experimental error of the sample at 21% porosity. With this in mind, Table IV shows that the temperature coefficients are practically constant independent of porosity. Thus, the thermal conductivity and electrical resistivity at any temperature may be computed by the following equations:

$$\frac{\lambda_T}{\lambda_{100}} = 1 + \alpha (T - 100) \quad (5)$$

$$\frac{\sigma_T}{\sigma_{100}} = 1 + \beta (T - 100) \quad (6)$$

where: $\alpha = \begin{cases} .00089 & \text{stainless steel} \\ -.000265 & \text{copper} \end{cases}$

$\beta = \begin{cases} .000544 & \text{stainless steel} \\ .00329 & \text{copper} \end{cases}$

3.4 DIMENSIONLESS CONDUCTIVITY AND RESISTIVITY

Using the thermal conductivity and electrical resistivity of solid material as a reference, the dimensionless thermal conductivity, $\frac{\lambda}{\lambda_0}$ and the dimensionless electrical resistivity, $\frac{\sigma_0}{\sigma}$ as a function of temperature for different porous material were computed from Tables II and III. The computed results are listed in Tables V, VI, and VII respectively for the stainless steel Rigimesh, the stainless steel powder, and the copper powders. An inspection of Tables V to VII reveals that the dimensionless thermal conductivity and electrical resistivity are essentially independent of temperature. This is consistent with the expressions of equations (5) and (6). Thus, an average value for each material and each porosity may be used in the subsequent discussions. These average values are shown in Figure 5. The solid lines in Figure 5 are represented by a correlation discussed in the following section.

3.4.1 Correlation of Dimensionless Conductivity and Resistivity.
 Different correlation equations have been published in the literatures (Ref. 2, 13-18). It has been found that the present experimental data can be best represented by either one of the following two equations:

$$\frac{\lambda}{\lambda_0} = \frac{1}{1 - \xi + \frac{1}{\frac{\alpha_0}{\xi} - \alpha_1}} \quad (7)$$

$$\frac{\lambda}{\lambda_0} = \frac{1 - \xi}{1 + n\xi^2} \quad (8)$$

Equation (7) was derived from a general form of the thermal conductivity of a mixture (References 13 and 14). Equation (8) was deduced from a porous material having different regular pore configurations (Reference 2). a_0 , a_1 and n are constants depending on the microstructure of the material and must be determined from experimental data.

Since equation (8) is significantly simpler than equation (7), it will be used in the present correlation. Equation (8) may be solved for n in terms of $\frac{\lambda}{\lambda_0}$ and ξ to yield:

$$n = \frac{1}{\xi^2} \left[\frac{1 - \xi}{\frac{\lambda}{\lambda_0}} - 1 \right] \quad (9)$$

Thus, using experimental data, n can be found for each pair of values of ξ and $\frac{\lambda}{\lambda_0}$. Using the results in Tables V, VI, and VII and excluding the Rigimesh and sintered stainless steel at about 9.2% porosity for the reason that there may be experimental errors, it was found that the value of n varies from 8.1 to 12.2 and the mean value for n is 10.2. Therefore, a round number of 10 will be used for n and the dimensionless conductivity is given by

$$\frac{\lambda}{\lambda_0} = \frac{1 - \xi}{1 + 10\xi^2} \quad (10)$$

Similarly, the correlation of electrical resistivity is given by:

$$\frac{\rho_0}{\rho} = \frac{1 - \xi}{1 + 11\xi^2} \quad (11)$$

Equations (10) and (11) are shown as solid lines in Figure 5. Considering the complexity of the problem and the significant differences in microstructures from Rigimesh to sintered powders, it is concluded from Figure 5 that the correlation is satisfactory. Whether or not this correlation is satisfactory for other microstructures, such as foam metal, felt metal, lamillcoy, poroloy, etc., remains to be substantiated.

3.4.2 Other Correlations and Experimental Data. It was shown in Reference 1 that for sintered matrices, the experimental data on thermal conductivity can be best correlated by a simple straight line as follows:

$$\frac{\lambda}{\lambda_0} = 1 - 2.1\xi \quad (12)$$

An extensive review of literature on thermal conductivity of porous materials performed in Reference 19 shows that equation (12) indeed represents the available experimental data well. This correlation, together with equation (10) and the model of parallel cylinders, $\frac{\lambda}{\lambda_0} = 1 - \xi$ are shown in Figure 6. Some experimental data are also shown in the Figure for comparison. However, for clarity, the experimental data for sintered powders compiled in References 1 and 19 are not shown in the figure.

Figure 6 shows that the equation $\frac{\lambda}{\lambda_0} = \frac{1-\xi}{1+10\xi}$ correlates all the experimental data very well. On the other hand, the parallel cylinder model, $\frac{\lambda}{\lambda_0} = 1 - \xi$ would over estimate the conductivity while the correlation $\frac{\lambda}{\lambda_0} = 1 - 2.1\xi$ would under estimate the conductivity when the porosity is larger than 30%.

Figure 6 shows also that the conductivity for Foametal and Feltmetal at high porosity ($\xi \geq 42\%$) can be represented by equation (10). No experimental data for these materials at low porosities are available to substantiate the correlation.

3.5 RELATION BETWEEN THERMAL CONDUCTIVITY AND ELECTRICAL RESISTIVITY

3.5.1 Relation Established in Literatures. Published literatures (Reference 23) show that within the temperature range where there is no magnetic transformation the thermal conductivity and electrical resistivity of solid materials are approximately related by the following Wiedermann-Franz-Lorenz equation

$$\lambda = \frac{LT}{\rho} + b \quad (13)$$

where L = Lorenz constant

$\frac{LT}{\rho}$ = Electronic component of thermal conductivity

b = Lattice component of thermal conductivity

Values of L and b for different materials can be found in Reference 23.

3.5.2 λ vs. $\frac{T}{\rho}$ of Present Data. Using the data in Tables II and III, the functional relationship between λ and $\frac{T}{\rho}$ for the present data is shown in Figures 7, 8, and 9 for the stainless Figimesh, stainless powders, and copper powders respectively. For the stainless steel materials, Figures 7 and 8 show that distinct straight lines could be drawn through the data for each porosity. Also, the slope is essentially the same between different lines and independent of porosity. Therefore, for the stainless steel material, the Lorenz constant in equation (13) is indeed a constant independent of porosity while the lattice component of conductivity b depends on the porosity. For the copper material, Figure 9 shows that all the data can be satisfactorily represented by a single line independent of porosity. Using a linear method, the line represents best the experimental data as follows:

$$\lambda = 2.307 \times 10^{-8} \frac{T}{\phi} + 18.6 \text{ (Copper Powders)} \quad (14)$$

In Reference 1 it is shown that the thermal conductivity and electrical resistivity of bronze powders can be represented by the following relation independent of porosity.

$$\lambda = 2.43 \times 10^{-8} \frac{T}{\phi} + 2.1 \text{ (Bronze Powders)} \quad (15)$$

So far, the available experimental data for porous materials show that:

- (1) The Wiedermann-Franz-Lorenz relation given by equation (13) is valid.
- (2) The Lorenz constant L depends on the kind of material and independent of porosity.
- (3) The lattice component of conductivity b depends on the kind of material for bronze and copper. It depends on the porosity as well for the stainless steel.

To explain the different dependency of b on porosity, the following information on conductivities of porous copper, bronze, and stainless steel Rigimesh at 50°C - 100°C is provided.

Material	Porosity	Conductivity				Source
		λ W-m ⁻¹ K ⁻¹	λ_e (LT/ρ)	λ_p (b)	$\frac{\lambda_p}{\lambda}$	
Copper at 100°C	.3009	163	144	18.6	.114	Present
Bronze at 50°C	.368	15.1	13	2.1	.14	Ref. 1
Stainless Steel at 100°C	.385	4.3	2.65	1.65	.384	Present

The above table shows that for porous bronze and copper, the lattice component of thermal conductivity is relatively unimportant (up to 14% of total conductivity) while for porous stainless steel Rigimesh, the lattice component of conduction (38%) is almost as important as the electronic component of conduction. Therefore, it is appropriate to postulate that within the temperature range where there is no magnetic transformation the lattice component of conduction depends on the porosity for all the materials. But, due to the limit in experimental accuracy, the effect of porosity on the lattice component of conductivity (i.e., b in equation 13) can only be found in low conductivity materials where the lattice conductivity is important and can not be found in high conductivity materials where the lattice conductivity is relatively

unimportant. For engineering applications, it may be stated that for bronze and higher conductivity materials, the thermal conductivity and resistivity is related by a single line of equation (13) with a single slope L and a single intercept b independent of porosity. For stainless steel and low conductivity materials, the thermal conductivity and electrical resistivity is related by a set of straight lines.

3.5.3 Correlation of λ vs. $\frac{T}{\rho}$ for 304L Stainless Steel Rigimesh. The experimental data on thermal conductivity and electrical resistivity at different temperatures and porosities are correlated to a single equation by the following postulation:

- (1) The slope L in equation (13) is a constant independent of porosity.
- (2) The lattice component of conductivity b is a linear function of porosity, i.e.,

$$b = C_0 - C_1 \rho$$

Thus, equation (13) can be rewritten as

$$\lambda = L \frac{T}{\rho} + C_0 - C_1 \rho \quad (16)$$

The constants, L, C_0 , and C_1 are found by the following steps:

- (1) For each porosity, determine the best slope L by a least square method.
- (2) All the values of L found in Step (1) are added and divided by the number of porosities. The result is taken as the best value for L.
- (3) Using the best value of L in equation (16) and the experimental data of λ , $\frac{T}{\rho}$, and ρ , the best values of C_0 and C_1 are determined by the least square method.

The resulting equation as found by the foregoing calculations for the 304L stainless steel Rigimesh is as follows:

$$\lambda + 9.236 \rho = 2.292 \times 10^{-8} \frac{T}{\rho} + 5.309 \text{ (Rigimesh)} \quad (17)$$

Figure 10 shows a comparison between the experimental data and the correlation. With the exceptions of two data points that deviate from the correlation equation by 6.6%, over 70% of the data fall within 3% of the correlation given by equation (17).

3.5.4 Correlation of λ vs. $\frac{T}{\rho}$ for 304L Stainless Steel Powders. The same procedures outlined in the foregoing section have been employed to correlate the data for the 304L stainless steel powders. The resulting equation is shown below.

$$\lambda + 13.56 \xi = 2.003 \times 10^{-8} \frac{T}{\rho} + 6.624 \quad (\text{Powders}) \quad (18)$$

A comparison of the correlation line and the experimental data is shown in Figure 11. The maximum deviation between the line and the experimental data is 5%; over 75% of the data are within 2% of the correlation. Thus correlation for the powders appear to be better than that for the Rigimesh.

3.5.5 Correlation of λ vs. $\frac{T}{\rho}$ for 304L Stainless Steel Rigimesh and Powders. When the data for both the Rigimesh and powders are considered together, the following correlation is obtained:

$$\lambda + 11.18 \xi = 2.16 \times 10^{-8} \frac{T}{\rho} + 5.956 \quad (19)$$

This correlation is shown in Figure 12 together with the experimental data. The maximum deviation between the correlation line and the experimental data is 9% for the Rigimesh at .093 porosity. Over 70% of the data fall within 5% of the value given by equation (19). In view of the complexity of the problem, this correlation is deemed satisfactory.

4.0 PREDICTION OF THERMAL CONDUCTIVITY OF POROUS MATERIALS

In general, the thermal conductivity and electrical resistivity of a solid material can be found in the literatures. This information may be used to estimate the thermal conductivity of the material at different porosity and temperature.

4.1 PREDICTION OF POROUS MATERIAL CONDUCTIVITY FROM SOLID CONDUCTIVITY DATA

When the thermal conductivity of solid material as a function of temperature is known, the thermal conductivity of porous material can be computed by use of equation (10). When the thermal conductivity of solid material is known only at a certain temperature, the thermal conductivity of porous material at any other temperature may be found by first computing the solid material conductivity from an equation similar to equation (5) and then obtain the answer by use of equation (10).

4.2 PREDICTION OF POROUS MATERIAL CONDUCTIVITY FROM ELECTRICAL RESISTIVITY DATA

When the electrical resistivity of a solid material as a function of temperature is given, the thermal conductivity of porous material can be found by two steps:

- (1) Determine the thermal conductivity of solid material as a function of temperature by use of equation (13) with appropriate constants L and b.

- (2) Compute the thermal conductivity of porous material by use of equation (10).

When the electrical resistivity of a solid material is known at a temperature only, the thermal conductivity at the same temperature can be found by use of equation (13). Equation (5) can then be used to determine the solid conductivity at any other temperature. Finally, the thermal conductivity of the material at a specific porosity can be computed by use of equation (10).

A numerical example of the computational procedure as outlined above is presented in Appendix A.

5.0 CONCLUSIONS AND RECOMMENDATIONS

5.1 CONCLUSIONS

Thermal conductivity and electrical resistivity of stainless steel Rigimesh, stainless steel powders and copper sintered spherical-powders at different porosities have been measured for a temperature range from 100°C up to 1000°C. Data have been analyzed and correlated. The correlations were tested using existing data for other porous materials. Based on this study, the following conclusions may be drawn.

- (1) For sintered powder and Rigimesh, the dimensionless thermal conductivity

can be represented by $\frac{\lambda}{\lambda_0} = \frac{1 - \xi}{1 + 10\xi^2}$ and the dimensionless electrical

resistivity is given by $\frac{\rho_0}{\rho} = \frac{1 - \xi}{1 + 11\xi^2}$. The correlation also fits the

existing data on thermal conductivity of foametal, feltmetal, and non-spherical sintered powders.

- (2) Within the temperature range where there is no magnetic transformation, the thermal conductivity of porous metals is related to the electrical resistivity and temperature by the Wiedermann-Franz-Lorenz equation:

$$\lambda = \frac{LT}{\rho} + b. \text{ For a high conductivity material, such as bronze and}$$

copper, where the lattice component of conduction is relatively unimportant the slope L and the intercept b are a function of material but independent of porosity. However, this intercept depends on the porosity as well as low conductivity material such as stainless steel where the lattice component of conductivity is almost as important as the electronic component of conductivity.

- (3) For Rigimesh and sintered powder structures, the thermal conductivity of porous materials can be computed from the information of solid material conductivity or solid material electrical resistivity.

5.2 RECOMMENDATIONS

This study has been limited to the porous Rigimesh and sintered powder structure. It is unknown whether or not the conclusions are valid for other microstructure of porous materials, such as feltmetal, at low porosity, foametal at low porosity, lamillloy, poroloy, etc. It is, therefore, suggested that study be extended to such different microstructures commonly used in engineering processes.

6.0

REFERENCES

1. P. Grootenhuis, R. W. Powell, and R. P. Tye, "Thermal and Electrical Conductivity of Porous Metal Made by Powder Metallurgy Methods," Proc. Phys. Soc., B 65 (1952) 502-511.
2. M. I. Aivazov and I. A. Domashnev, "Influence of Porosity on the Conductivity of Hot-Pressed Titanium-Nitride Specimens," Institute for New Chemical Problems, Academy of Sciences of the USSR. Translated from Poroshkovaya Metallurgiya No. 9, (69), pp 51-54, September 1968.
3. R. E. Regan, "Characterization of Porous Matrices for Transpiration Cooled Structures," NASA CR-72699 (1970).
4. G. Friedman, "Fabrication, Characterization and Thermal Conductivity of Porous Copper and Stainless Steel Materials," NASA CR 72755 (1971).
5. R. E. Regan, "Characterization of Porous Powder Metal Matrices for Transpiration Cooled Structures," NASA CR 72994 (1971).
6. R. P. Tye, "An Experimental Investigation of the Thermal Conductivity and Electrical Resistivity of Three Porous 304L Stainless Steel "Rigimesh" Material to 1300°K", NASA CR-72710 (1970).
7. Aerospace Structural Metals Handbook, ASD-TDR-63-741, Vol. I, 1963. Air Force Materials Laboratory, Wright Patterson Air Force Base, Ohio.
8. Argonne National Laboratory, ANL-5914, September 1958, p. 64.
9. ASTM Special Technical Publication, No. 296, p. 67.
10. Metals Handbook, 8th Edition, Vol. 1, Properties and Selection, American Society for Metals, page 422.
11. Y. S. Touloukian, "Thermophysical Properties of High Temperatures Solid Materials," Vol. I, III, MacMillan Company, New York, (1967).
12. A. Cezairliyan and Y. S. Touloukian, "Prediction of Thermal Conductivity of Metals," 3rd Conference on Thermal Conductivity, Oak Ridge National Laboratory, Oak Ridge, Tennessee (1963). pp. 3-19.
13. D. A. G. Bruggeman, "Dielectric Constant and Conductivity of Mixtures of Isotropic Materials," Annalen Physik, Vol. 24, 1935, pp. 636-679.
14. A. E. Powers, "Fundamentals of Thermal Conductivity at High Temperatures," Knolls Atomic Power Laboratory, Report No. KAPL-2143, April 7, 1961.
15. V. V. Skorokhod, "Electrical Conductivity, Modulus of Elasticity and Viscosity Coefficients of Porous Bodies," Powder Metallurgy, 1963. No. 12, p. 188-200.

16. A. V. Kuikov, A. T. Shashkov, L. L. Vasiliev, and Yu. E. Fraiman, "Thermal Conductivity of Porous Systems," Int. J. Heat Mass Transfer, Vol. II, pp 117-140 (1968).
17. S. Masamune and J. M. Smith, "Thermal Conductivity of Beds of Spherical Particles," I & EC Fundamentals, Vol. 2, No. 2 (1963), pp 136-142.
18. S. C. Cheng and R. I. Vachon, "A Technique for Predicting the Thermal Conductivity of Suspensions, Emulsions and Porous Materials," Int. J. Heat Mass Transfer, Vol. 13, pp 537-546 (1970).
19. "Investigation of Methods for Transpiration Cooling Liquid Rocket Chambers," Pratt & Whitney Aircraft, PWA FR-3390 (1969).
20. J. D. McClelland, "Materials and Structures Physical Measurements Program," Report Number TDR-930 (2240-64) TR-1, Aerospace Corporation (1962).
21. J. C. Y. Koh, E. P. del Casal, R. W. Evans, and V. Deriugin, "Fluid Flow and Heat Transfer in High Temperature Porous Matrices for Transpiration Cooling," AFFDL-TR-66-70 (1966).
22. J. E. Evans, Jr., "Thermal Conductivity of 14 Metals and Alloys Up to 1100°F," NACA RM E50L07 (1951).
23. R. W. Powell, "Correlation of Metallic Thermal and Electrical Conductivities for Both Solid and Liquid Phases," Int. J. Heat Mass Transfer, Vol. 8, pp 1033-1045 (1965).

NOMENCLATURE

a_0, a_1	Constants, equation (7)
b	Constant in Wiedermann-Franz-Lorenz equation
c_0, c_1	Constants, equation (16)
L	Constant in Wiedermann-Franz-Lorenz equation
n	Constant, equation (8)
T	Temperature
α	Temperature coefficient for conductivity, equation (5)
β	Temperature coefficient for resistivity, equation (6)
λ	Thermal conductivity
σ	Electrical resistivity
ξ	Porosity

Subscripts

0	Solid material ($\xi = 0$)
l	Lattice component
e	Electronic component

TABLE I DETAILS OF TESTED SAMPLES

No.	Materials	Porosities	Size mm	λ or ρ	Flow \perp or \parallel to Weave Pattern
1	304L SS Rigimesh	.093	63.9x63.8x20.6	λ	\perp
2	304L SS Rigimesh	.093	6.36 x 6.26x20.11	ρ	\perp
3	304L SS Rigimesh	.093	6.22x6.30x59.46	ρ	\parallel
4	304L SS Rigimesh	.203	64.4x64.6x26.19	λ	\perp
5	304L SS Rigimesh	.203	6.55x6.26x26.32	ρ	\perp
6	304L SS Rigimesh	.203	6.70x6.19x58.71	ρ	\parallel
7	304L SS Rigimesh	.385	62.75x62.59x24.46	λ	\perp
8	304L SS Rigimesh	.385	6.64x6.45x25.52	ρ	\perp
9	304L SS Rigimesh	.385	6.73x6.60x59.07	ρ	\parallel
10	304L SS Sintered Powder	0	25.5(d) x 25.4 (1)	λ	
11	304L SS Sintered Powder	0	6.45 (d) x 31.5 (1)	ρ	
12	304L SS Sintered Powder	.92	25.6 (d) x 26.3 (1)	λ	
13	304L SS Sintered Powder	.928	6.39 (d) x 42.4 (1)	ρ	
14	304L SS Sintered Powder	.2138	25.6 (d) x 25.4 (1)	λ	
15	304L SS Sintered Powder	.2158	6.40 (d) x 26.6 (1)	ρ	
16	304L SS Sintered Powder	.310	25.4 (d) x 25.2 (1)	λ	
17	304L SS Sintered Powder	.3199	6.30 (d) x 40.1 (1)	ρ	
18	OFHC Copper Sintered Powder	0	25.4 (d) x 25.4 (1)	λ	
19	OFHC Copper Sintered Powder	0	6.35 (d) x 31.1 (1)	ρ	
20	OFHC Copper Sintered Powder	.1031	25.1 (d) x 25.4 (1)	λ	
21	OFHC Copper Sintered Powder	.1031	6.35 (d) x 42.2 (1)	ρ	
22	OFHC Copper Sintered Powder	.2096	25.4 (d) x 25.4 (1)	λ	
23	OFHC Copper Sintered Powder	.2096	25.4 (d) x 25.4 (1)	ρ	
24	OFHC Copper Sintered Powder	.3009	25.5 (d) x 25.4 (1)	λ	
25	OFHC Copper Sintered Powder	.3077	6.27 (d) x 38.9 (1)	ρ	

TABLE II

Thermal Conductivity, λ W m⁻¹ deg⁻¹; 10⁸ x Electrical Resistivity, ρ
 ohm m AND DERIVED 10⁸ x LORENZ FUNCTION, L, V² deg K⁻² FOR POROUS 304L STAINLESS STEEL

(a) "RIGIMESH"

Porosity %	Temperature K	.093			.203			.385				
		λ	ρ	L	f_{II}^*	λ	ρ	L	f_{II}^*	λ	ρ	L
373	13.7	100	3.68	94	8.6	159	3.67	130	4.3	327	3.76	221
573	16.2	117	3.31	110.2	10.1	187	3.30	152.5	5.1	384	3.41	255
773	18.9	130	3.18	122.8	11.6	208.5	3.13	170	5.8	424	3.18	287
973	21.5	140.5	3.11	132.7	13.0	225	3.02	184	6.55	451	3.03	307
1173	24.2	148.5	3.06	140.2	14.4	237.5	2.92	194.5	7.3	478	2.97	328
1273	25.4	152	3.03	144	15.2	243	2.90	199.5	7.6	492	2.93	338

* ρ is the electrical resistivity for current flow parallel to the weave pattern.
 All other quantities are for flow perpendicular to the weave direction.

TABLE II Continued

(b) SINTERED POWDERS

POROSITY	0	.092	.0328	.2138	.2158	.31	.3195	
TEMPERATURE, K	$10^8 \gamma$	$10^8 L$	λ	$10^8 \gamma$	$10^8 L$	λ	$10^8 \gamma$	$10^8 L$
373	16.3	78.8	3.44	11.5	112	3.57	9.1	147.5
573	18.9	93.0	3.06	14.0	122	2.99	10.2	175
773	21.75	104.5	2.95	16.0	135	2.80	11.4	195
973	24.5	112.0	2.82	18.2	146	2.74	12.6	213
1173	27.3	116.5	2.72	20.4	157	2.72	13.7	231
							2.70	2.70
							9.6	9.6
							3.38	3.38
							2.76	2.76

TABLE III

THERMAL CONDUCTIVITY, λ , $\text{W m}^{-1} \text{deg}^{-1}$; $10^8 \times$ ELECTRICAL RESISTIVITY, ρ
 ohm m AND DERIVED 10^8 LORENZ FUNCTION, Λ , $\text{V}^2 \text{ deg K}^{-2}$ FOR COPPER SINTERED POWDERS

POROSITY: %	0			.1031			.103			.2096			.3009			.3077		
	Temperature, K	λ	$10^8 \rho$	$10^8 \Lambda$														
373	396	2.30	2.44	324	2.85	2.48	232	4.25	2.62	163	6.2	2.62	158	7.9	2.64			
473	389	3.00	2.47	315	3.70	2.47	221	5.6	2.61	154	9.8	2.64						
576	380	3.70	2.45	307	4.55	2.44	207	7.3	2.64	148	11.8	2.59	154	9.8	2.64			
673	370	4.45	2.44	297.5	5.40	2.39	197	9.0	2.63	143	13.7	2.54						
873	360	5.20	2.43	289	6.4	2.40	184	11.15	2.64	139	15.7	2.50						
973	351	6.02	2.43	280	7.4	2.37	172	13.1	2.58	-	-	-						
1073	342	6.9	2.43	271	8.75	2.44	160	15.1	2.49	-	-	-						

TABLE IV TEMPERATURE COEFFICIENTS

MATERIALS	POROSITY	TEMPERATURE RANGE (C)	α	β
Stainless	.093	100 - 1000	.000949	.000578
Rigimesh	.203 .385		.000853 .000853	.000587 .00056
Stainless	0	100 - 900	.000844	.000598
Powders	.0924 .2148 .315		.000893 .000632 .000932	.000502 .000708 .00044
Copper	0	100 - 700	-.000227	.00333
Powders	.1031 .2096 .3043		-.000273 -.000517 -.000294	.00345 .00425 .00309
Bronze	0 - .368	20 - 200	.0021	.00058
Powders			(50°C-200°C)	(20°C-200°C)
(Reference 1)				

TABLE V DIMENSIONLESS CONDUCTIVITY AND RESISTIVITY OF 304L STAINLESS STEEL RIGIMESH

POROSITY	.093	.203	.385
TEMPERATURE (K)	$\frac{\lambda}{\lambda_0}$	$\frac{\rho_0}{\rho}$	$\frac{\lambda}{\lambda_0}$
373	.840	.788	.528
573	.857	.795	.534
773	.869	.804	.533
973	.878	.797	.531
1173	.886	.784	.527
1273	<u>.885</u>	<u>.771</u>	<u>.530</u>
Average	.869	.790	.530
			.494

TABLE VI DIMENSIONLESS CONDUCTIVITY AND RESISTIVITY OF
304L STAINLESS STEEL SINTERED POWDER

POROSITIES	.092	.0928	.2138	.2158	.3138	.3199
TEMPERATURE (K)	$\frac{\lambda}{\lambda_0}$	$\frac{\rho_0}{\rho}$	$\frac{\Delta}{\lambda_0}$	$\frac{\rho_0}{\rho}$	$\frac{\lambda}{\lambda_0}$	$\frac{\rho_0}{\rho}$
373	.730	.704	.558	.534	.337	.315
573	.741	.762	.540	.531	.341	.320
773	.746	.774	.524	.536	.349	.332
973	.743	.767	.514	.526	.351	.337
1173	<u>.747</u>	<u>.742</u>	<u>.502</u>	<u>.504</u>	<u>.352</u>	<u>.345</u>
Average	.739	.750	.528	.526	.347	.330

TABLE VII DIMENSIONLESS CONDUCTIVITY AND RESISTIVITY OF
SINTERED POWDER COPPER

POROSITY (X)	.1031	.1031	.2096	.2096	.3009	.3077
TEMPERATURE (K)	$\frac{\lambda}{\lambda_0}$	$\frac{\rho}{\rho_0}$	$\frac{\lambda}{\lambda_0}$	$\frac{\rho}{\rho_0}$	$\frac{\lambda}{\lambda_0}$	$\frac{\rho}{\rho_0}$
373	.818	.807	.586	.541	.412	.371
473	.810	.811	.568	.536	.406	.380
573	.808	.813	.545	.507	.405	.378
673	.804	.824	.532	.494	.40	.377
773	.803	.812	.511	.466	.397	.380
873	.798	.814	.490	.460	.396	.383
973	.792	.789	.468	.451	—	.390
Average	.805	.810	.528	.494	.403	.380

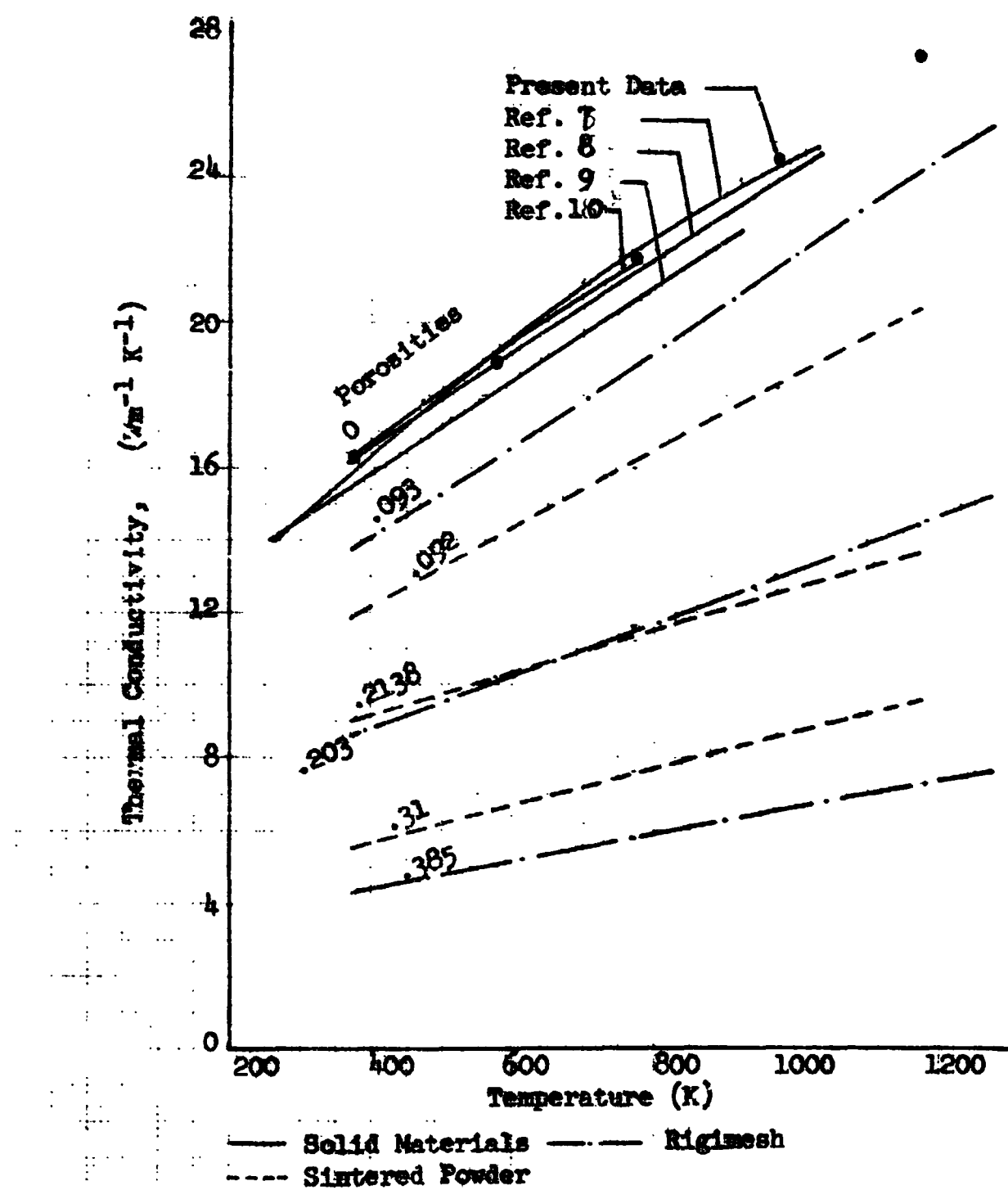


FIGURE 1. THERMAL CONDUCTIVITY OF POROUS 304 AND 304L STAINLESS STEEL

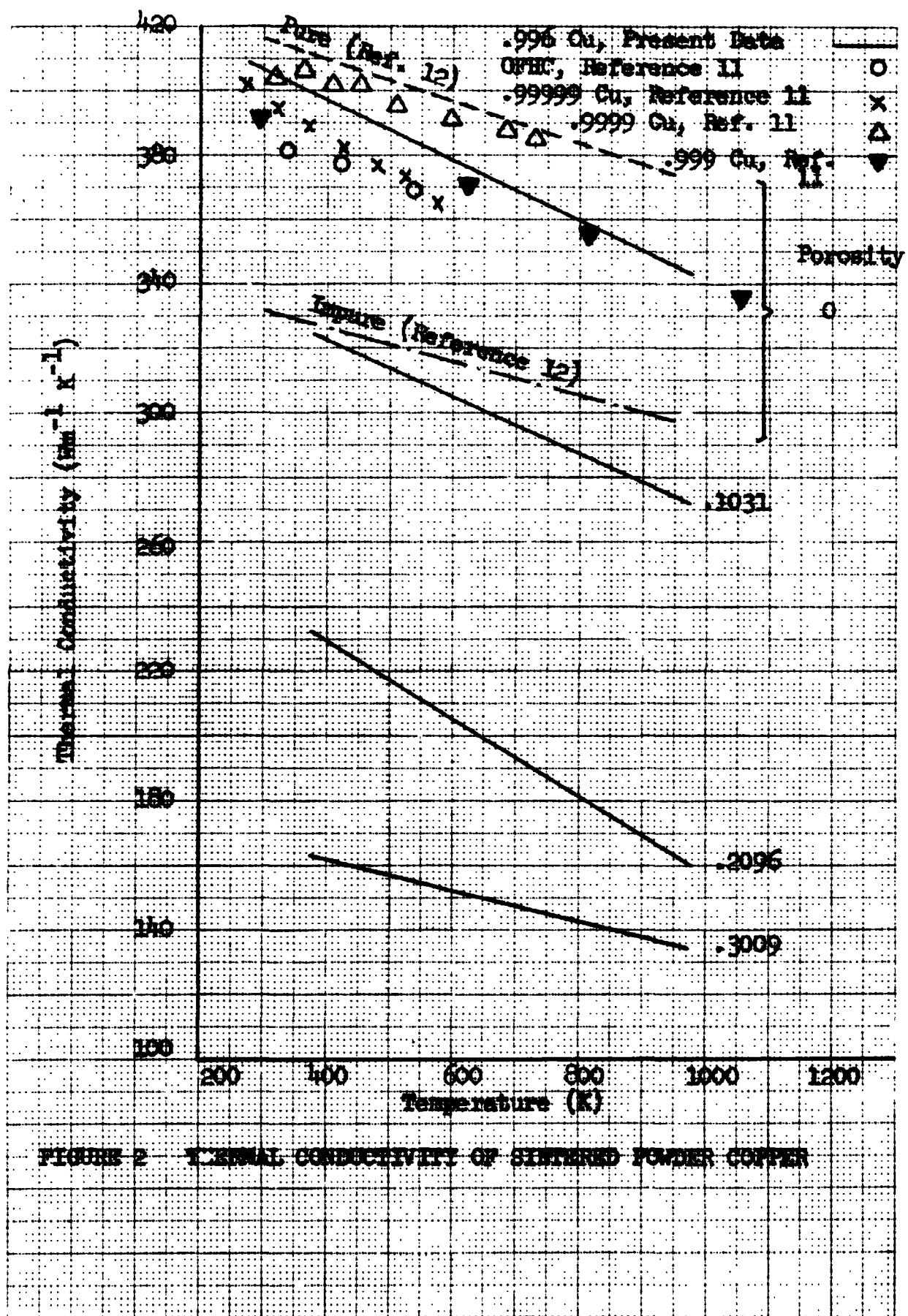
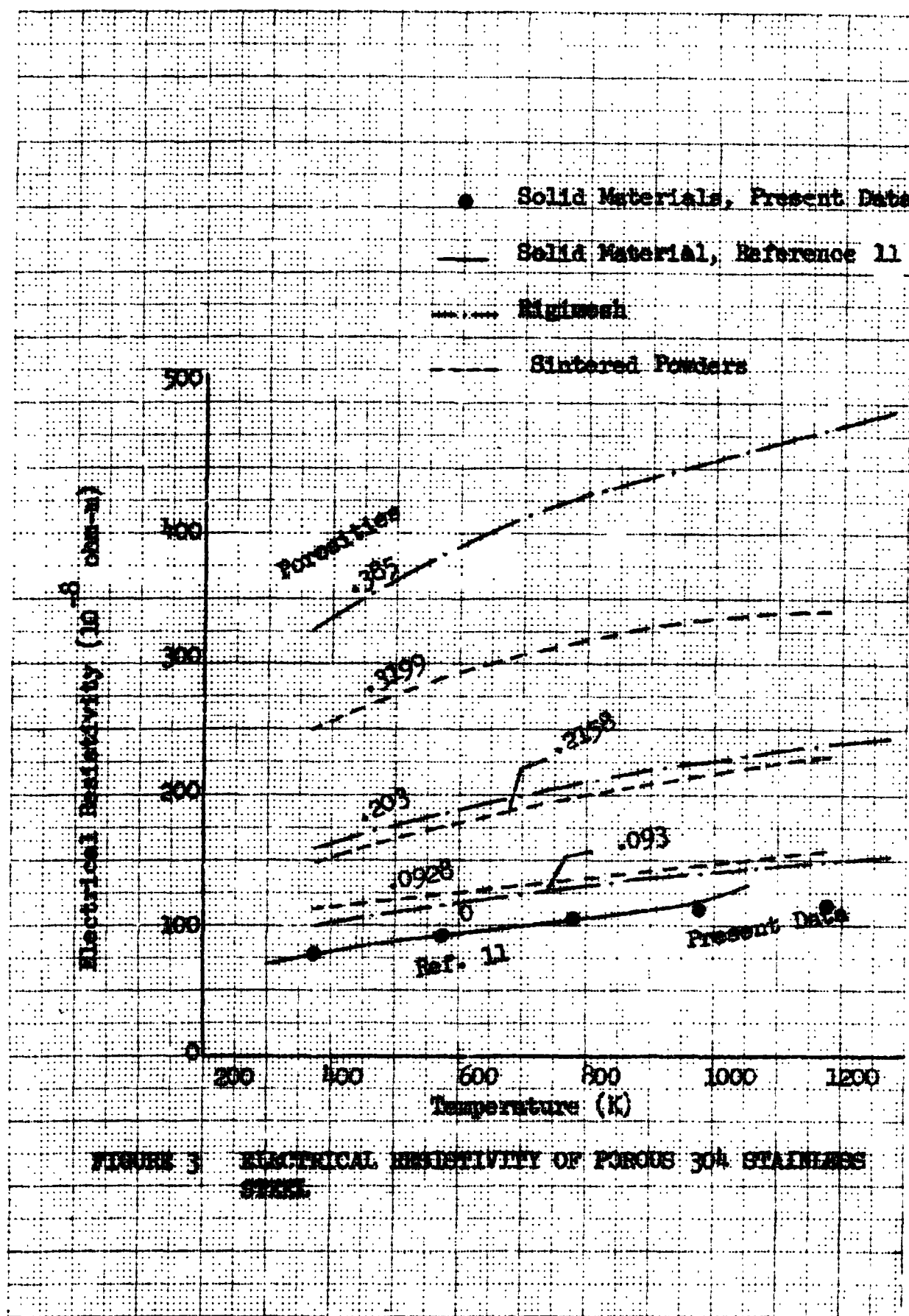


FIGURE 2 ELECTRICAL CONDUCTIVITY OF SINTERED POWDER COPPER



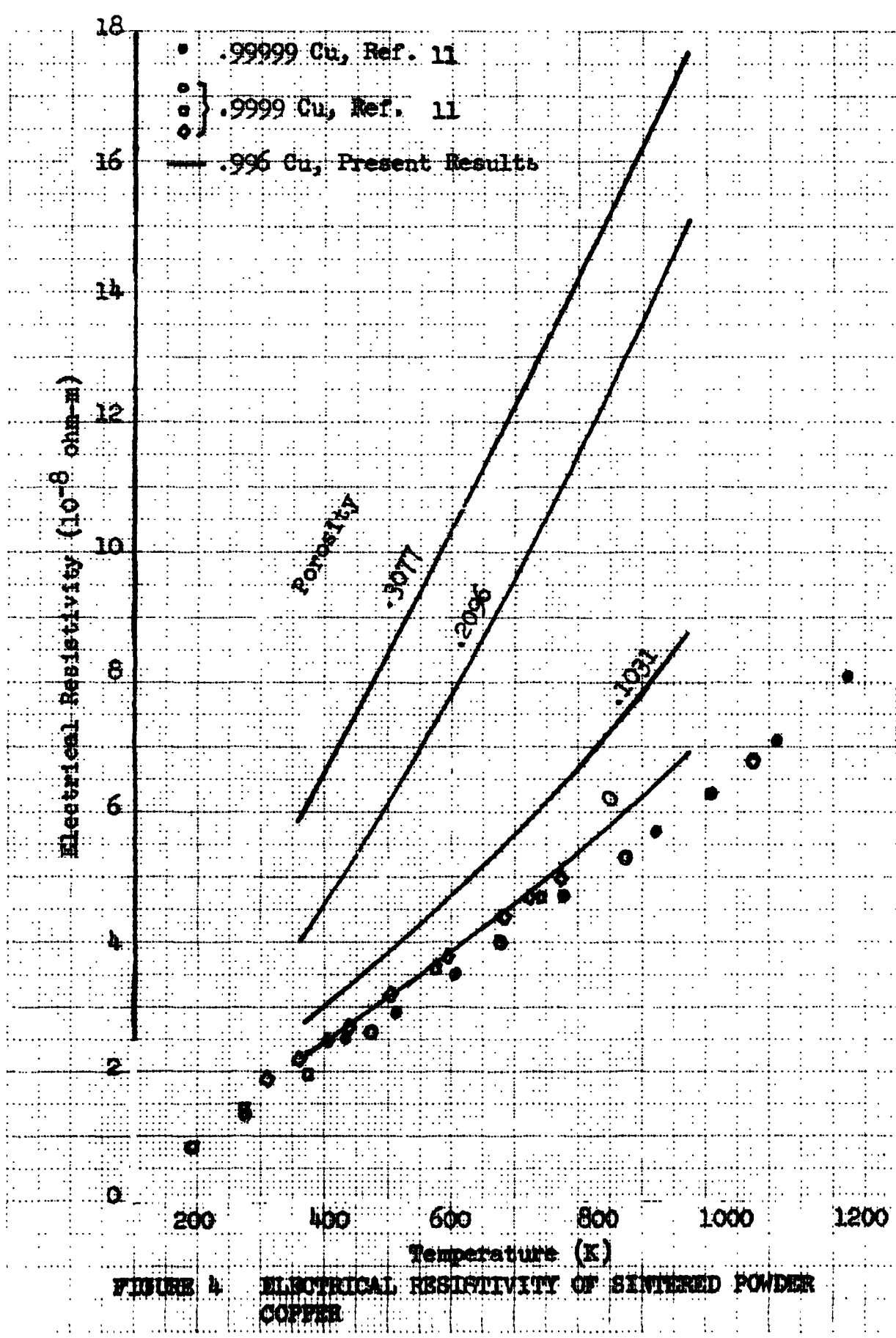


FIGURE 4. ELECTRICAL RESISTIVITY OF SINTERED POWDER COPPER

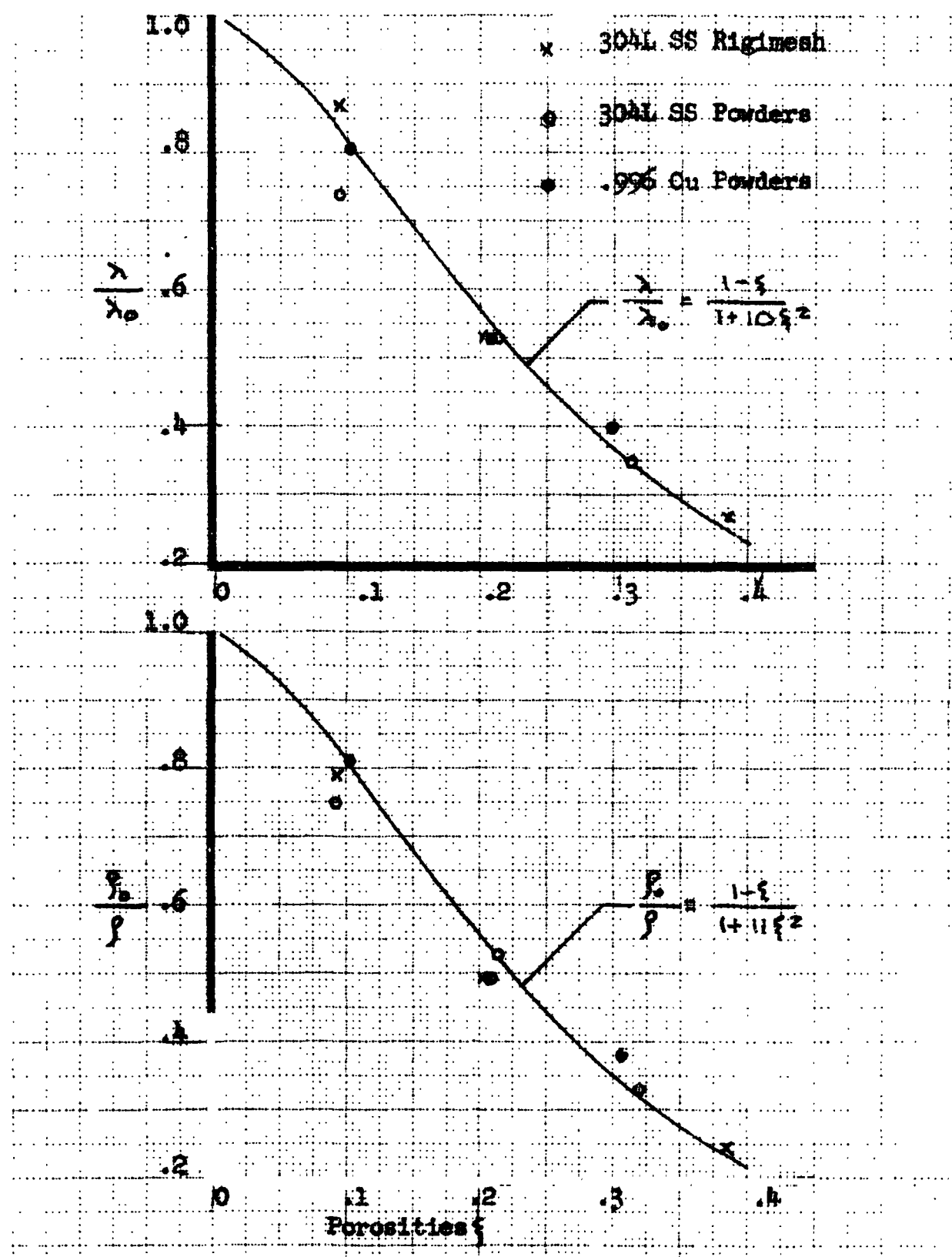


FIGURE 5. DIMENSIONLESS THERMAL CONDUCTIVITY, $\frac{\lambda}{\lambda_0}$, AND ELECTRICAL RESISTIVITY ρ/ρ_0 OF POROUS MATERIALS

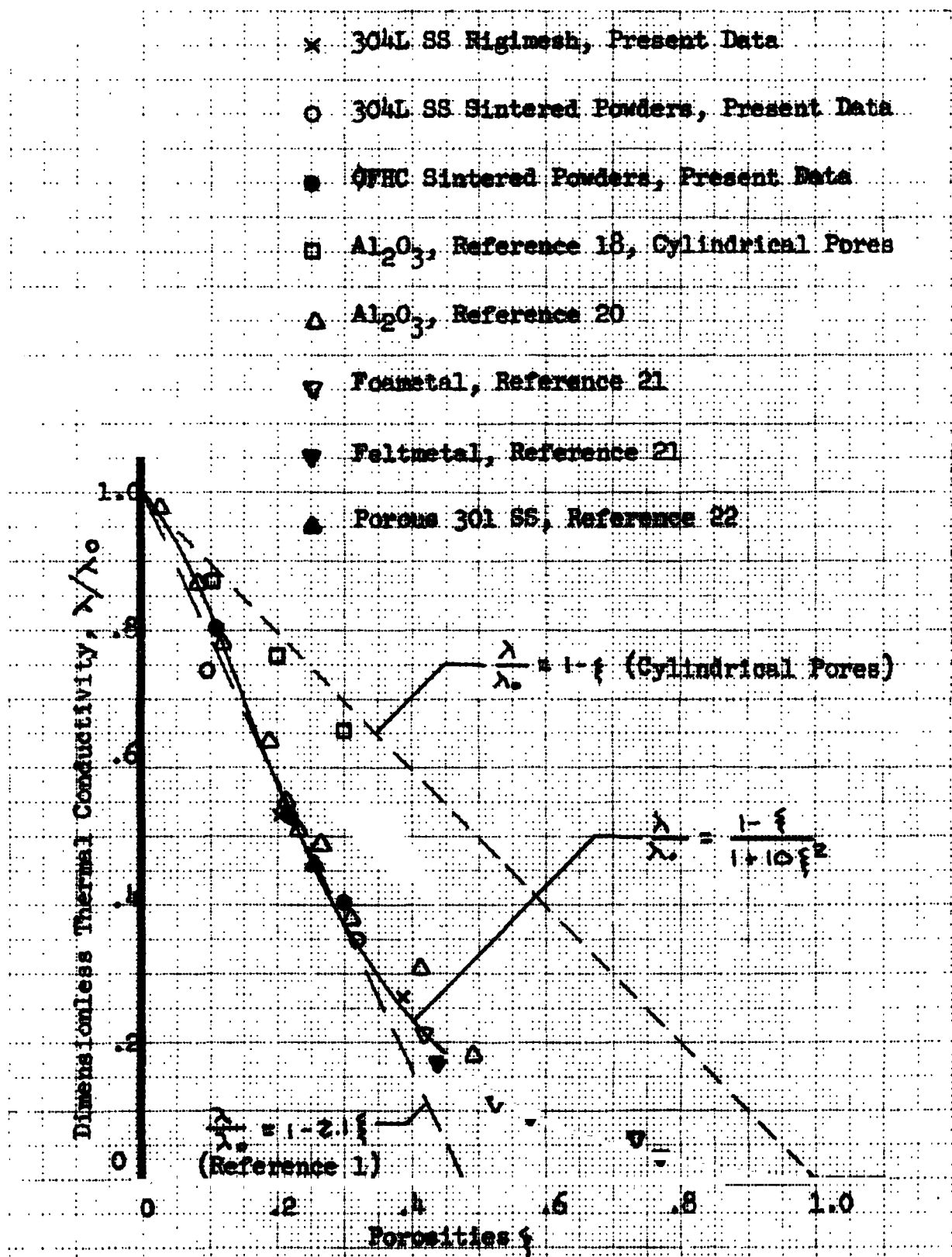
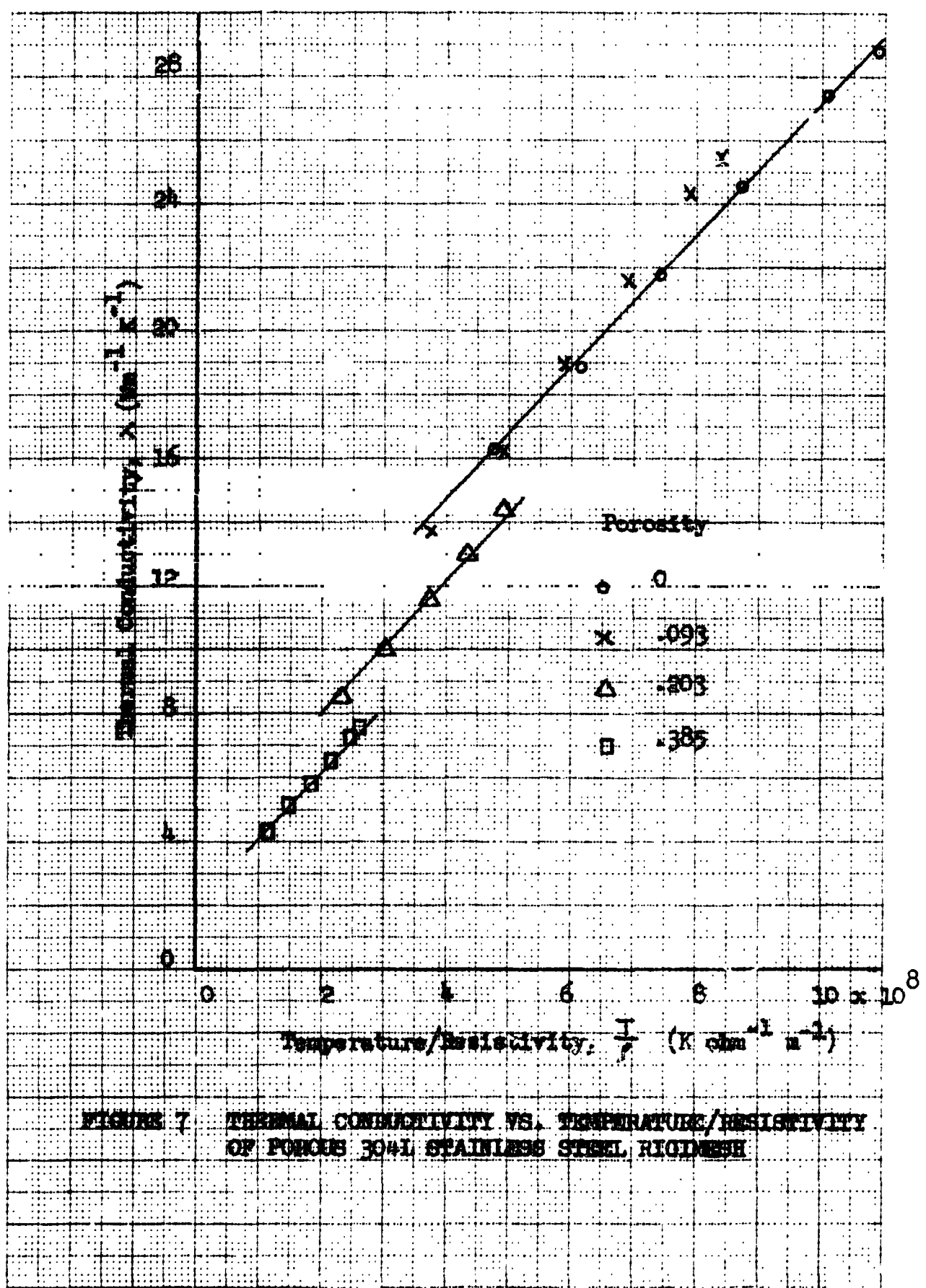
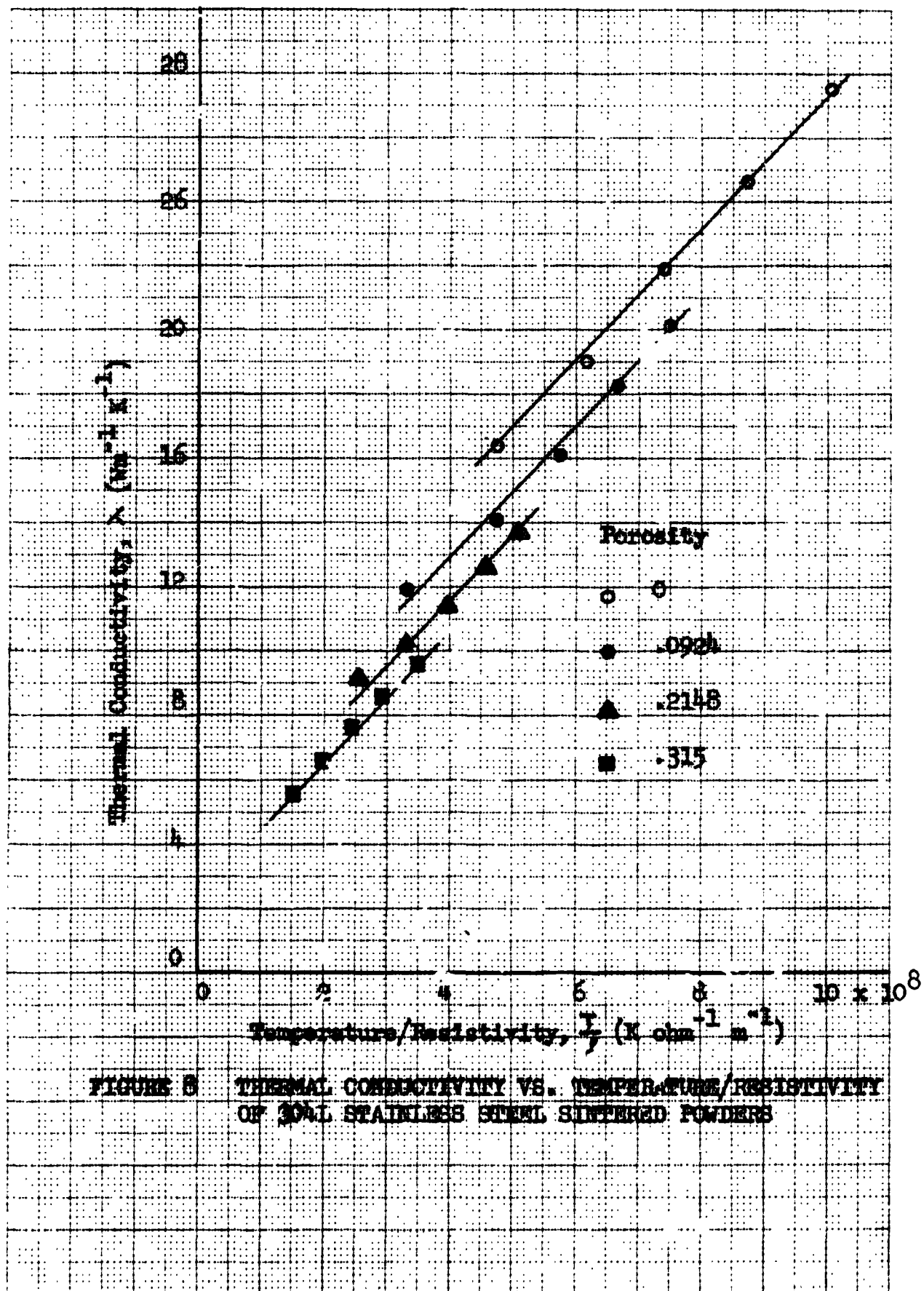


FIGURE 6 COMPARISON OF EXPERIMENTAL DATA ON CORRELATIONS OF THERMAL CONDUCTIVITY OF POROUS MATERIALS





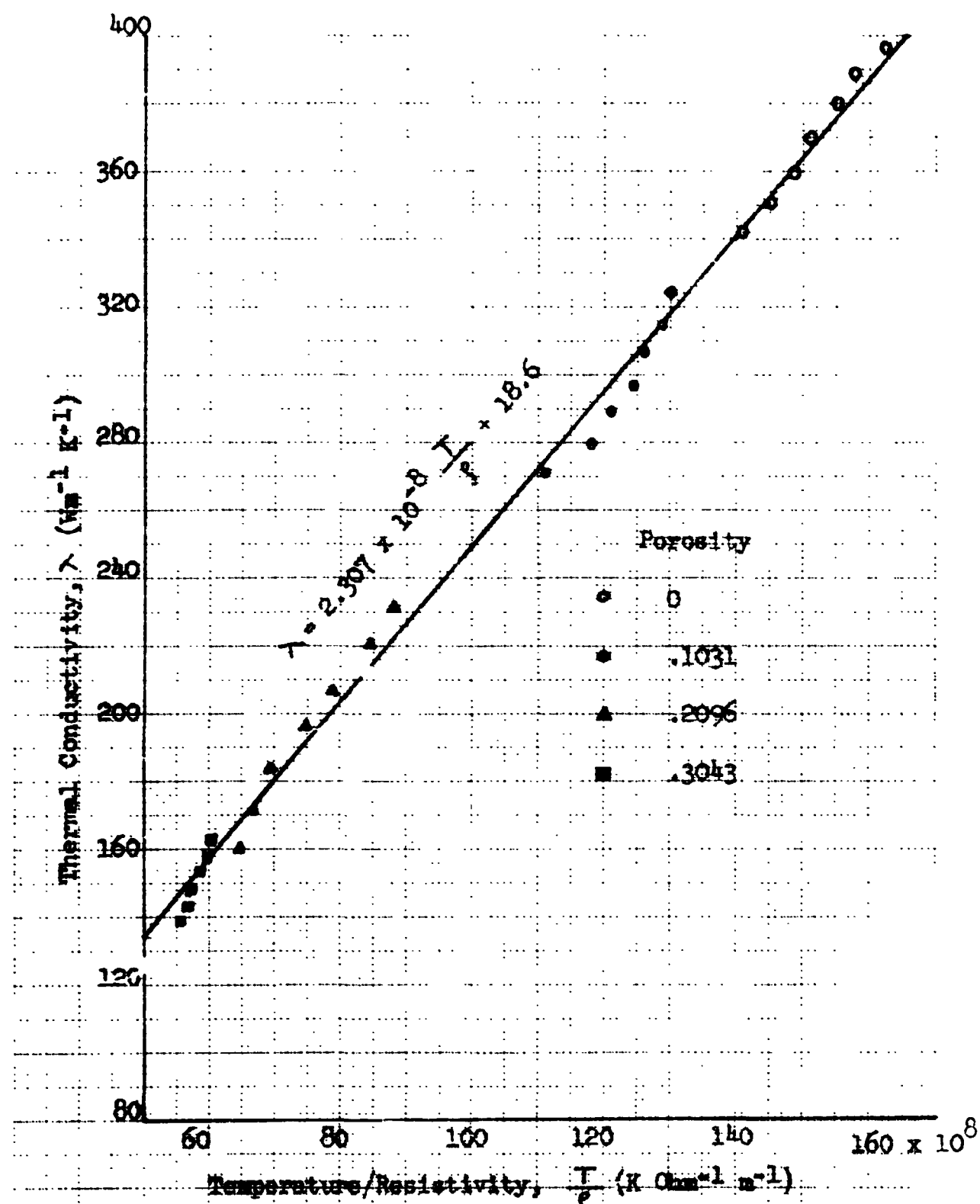
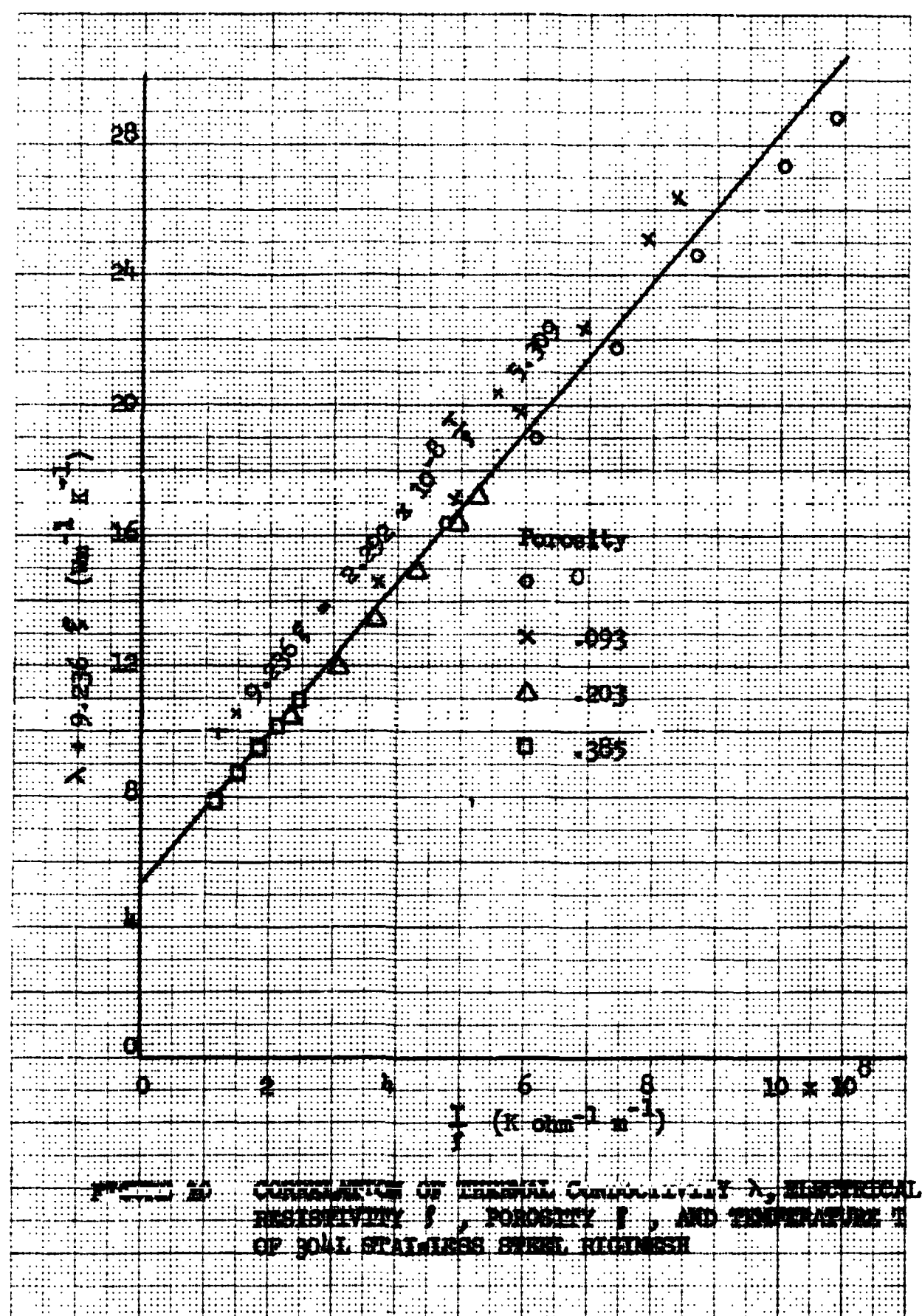
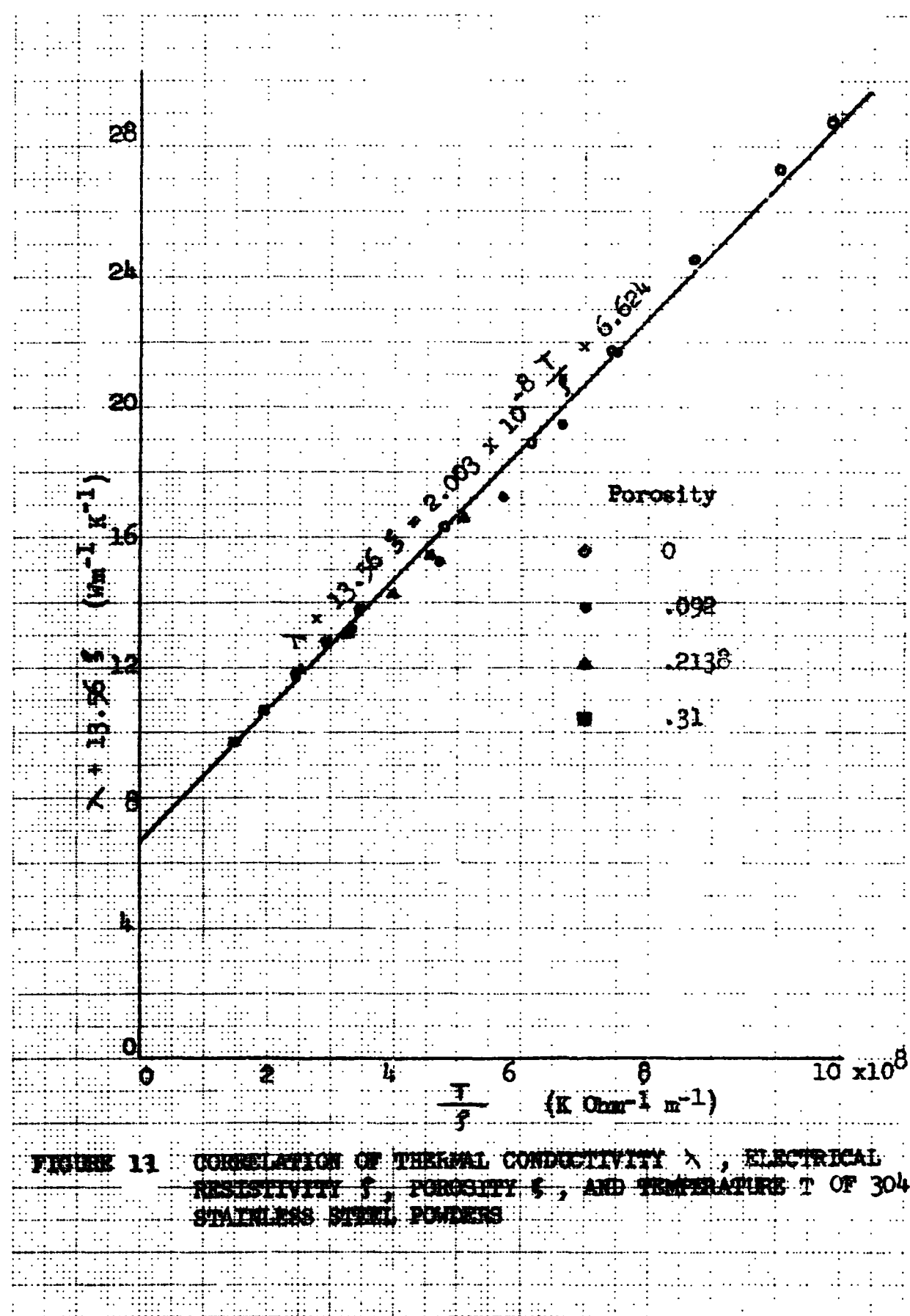


FIGURE 9 THERMAL CONDUCTIVITY VS. TEMPERATURE/RESISTIVITY OF OFEC SINTEKED POWDERS





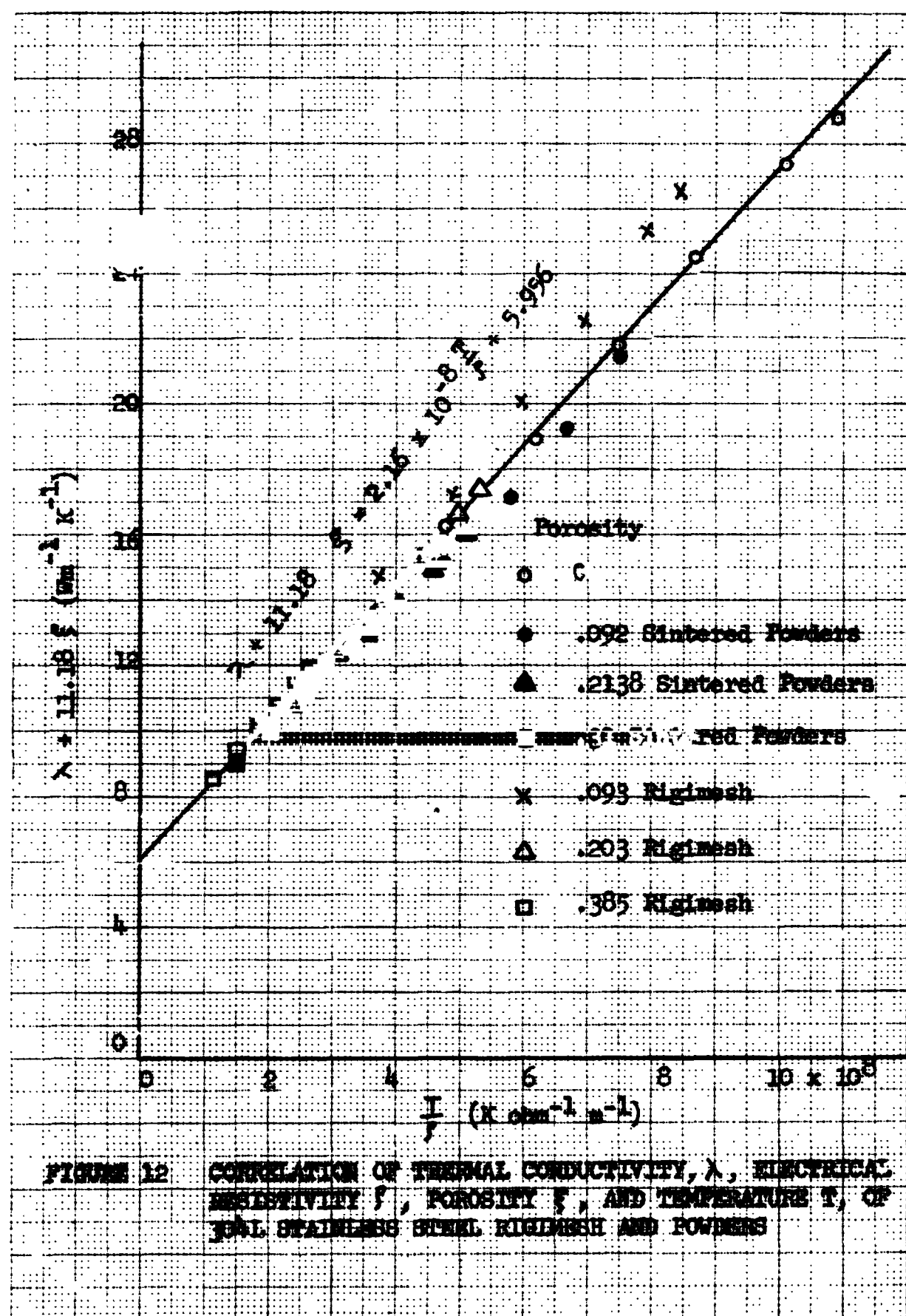


FIGURE 12 CORRELATION OF INTERNAL CONDUCTIVITY, λ , ELECTRICAL RESISTIVITY, ρ , POROSITY, ϕ , AND TEMPERATURE T , OF 316L STAINLESS STEEL REGIMESH AND POWDERS

APPENDIX A - NUMERICAL EXAMPLE

The computational procedures outlined in Section 4.0 are demonstrated in the following example where the conductivity of 304L stainless steel powders at 500°C having a porosity of 0.31 is to be computed from different known information.

(1) Given $\lambda_0 = 21.75 \text{ W m}^{-1} \text{ C}^{-1}$ at $T = 500^\circ\text{C}$ $\xi = 0$

From equation (10), the conductivity at 500°C and $\xi = .31$ is

$$\lambda = 21.75 \frac{1 - .31}{1 + 10 (.31)^2} = 21.75 (.35186) = 7.65$$

(2) Given $\lambda_0 = 16.3 \text{ W m}^{-1} \text{ C}^{-1}$ at $T = 100^\circ\text{C}$ $\xi = 0$

From equation (5), λ at 500°C and $\xi = 0$ is

$$\lambda_0 = 16.3 (1 + .00089 (500 - 100)) = 22.1 \text{ W m}^{-1} \text{ C}^{-1}$$

From equation (10), λ at 500°C and $\xi = .31$ is

$$\lambda = 22.1 \frac{1 - 0.31}{1 + 10 (.31)^2} = 7.78$$

(3) Given $\rho_0 = 104.5 \times 10^{-8} \Omega \cdot \text{m}$ at $T = 500^\circ\text{C}$, $\xi = 0$

From equation (19), the thermal conductivity λ_0 at 500°C and $\xi = 0$ is

$$\lambda_0 = 2.16 \times 10^{-8} \frac{500 + 273}{104.5 \times 10^{-8}} + 5.956 = 21.9$$

From equation (10), the thermal conductivity λ at 500°C and $\xi = .31$ is

$$\lambda = 21.9 \frac{1 - .31}{1 + 10 (.31)^2} = 7.71$$

(4) Given $\rho_0 = 78.8 \times 10^{-8} \Omega \cdot \text{m}$ at 100°C and $\xi = 0$

From equation (19), the thermal conductivity at 100°C and $\xi = 0$ is

$$\lambda_0 = 2.16 \times 10^{-8} \frac{100 + 273}{78.8 \times 10^{-8}} + 5.956 = 16.18 \text{ W m}^{-1} \text{ C}^{-1}$$

From equation (5), the thermal conductivity at 500°C and $\xi = 0$ is

$$\lambda_0 = 16.18 \left[1 + .00089 (400) \right] = 21.94 \text{ Wm}^{-1} \text{ C}^{-1}$$

From equation (10), the thermal conductivity λ at 500°C and $\xi = .31$ is

$$\lambda = 21.94 \frac{1 - .31}{1 + 10 (.31)^2} = 7.72$$

Measured value of thermal conductivity at 500°C and .31 porosity as given by Table II (b) is $7.6 \text{ Wm}^{-1} \text{ C}^{-1}$. Thus, the maximum deviation between the computed and measured results is 2.4%.